Theory of the anharmonic damping and shift of the Raman mode in silicon

E. Haro and M. Balkanski
Laboratoire de Physique des Solides de l'Université Pierre et Marie Curie, Tour 13, 4 place Jussieu, 75230 Paris Cédex 05, France

R. F. Wallis
*Laboratoire de Physique des Solides de l'Université Pierre et Marie Curie, Tour 13, 4 place Jussieu, 75230 Paris Cédex 05, France and Department of Physics, University of California, Irvine, California 92717**

K. H. Wanser
McDonnell Douglas Astronautics Corporation, 5301 Bolsa Avenue, Huntington Beach, California 92647
(Received 16 June 1986)

A theoretical investigation has been made of the damping constant and frequency shift of the Raman mode in silicon due to cubic anharmonic interactions between nearest-neighbor atoms. The normal-mode frequencies and eigenvectors for the harmonic crystal were calculated using a model containing short-range forces out to fourth neighbors and long-range nonlocal dipole interactions. The Raman-mode linewidth and frequency shift were calculated as functions of both temperature and frequency, and the results are compared with experimental data on the temperature dependences of these quantities.

I. INTRODUCTION

In recent years, a wealth of experimental information has been obtained on the optical modes of vibration of a wide variety of crystals using the inelastic scattering of light. Particularly important in pure materials are the optical modes at the center of the Brillouin zone. For these modes the line center and the linewidth of the scattered radiation are found to vary with temperature. Such a temperature dependence can be understood in terms of the anharmonic character of the lattice vibrations.[1]

A number of experimental investigations have been made of the temperature dependence of the light scattering spectrum of pure silicon. Hart, Aggarwal, and Lax[2] measured the frequency shift of the line center and the linewidth over the temperature range from 20 to 770 K. At temperatures above 300 K, both the frequency shift and linewidth were found to vary linearly with the absolute temperature T, a result consistent with theoretical predictions[1] based on cubic anharmonicity carried to second order in perturbation theory. Quantitatively, the results of Hart *et al.* for the frequency shift agree fairly well with the theoretical calculations of Cowley[3] based on cubic anharmonicity to second order, but their results for the linewidth are in significant disagreement with those of Cowley. However, the data of Hart *et al.* for the linewidth can be fitted satisfactorily by the cubic anharmonic model of Klemens,[4] if the zero-temperature value of the linewidth is chosen to agree with experiment.

A more extensive experimental investigation of the temperature dependence of the light scattering spectrum of optical phonons in silicon has been carried out by Balkanski, Wallis, and Haro[5] who reported measurements over the range 5 to 1400 K. As in the case of Hart *et al.*, the data for the linewidth do not agree well with the calculations of Cowley, but can be fit by the cubic anharmonic Klemens model at temperatures below 400 K. Above 400 K, both the frequency shift and linewidth increase more strongly with temperature than linearly, indicating that quartic anharmonic processes as well as higher order cubic anharmonic processes must be considered. Indeed, by extending the Klemens model to include the latter processes, a satisfactory fit to both the frequency shift and linewidth was achieved up to 1200 K. However, the fit was obtained by suitably choosing certain empirical constants and is therefore not the result of a proper lattice dynamical calculation. It is the purpose of the present paper to provide the latter.

Recently, Menéndez and Cardona[6] have reported additional measurements of the linewidth and line shift in silicon at temperatures up to ~ 800 K. Their results appear to be in substantial agreement with those of Balkanski *et al.*[5] Menéndez and Cardona infer that the principal decay channel at not overly high temperatures involves the creation of LA-LO phonon pairs rather than two phonons in the same branch as in the Klemens model. They also infer that the discrepancies between the experimental data and Cowley's calculations are largely due to the inadequacies of the shell model used by Cowley.

As is evident from the foregoing discussion, the principal theoretical calculation that has been made to date of the linewidth and line shift in silicon is that of Cowley.[3] For the harmonic part of the lattice dynamical model, Cowley used a shell model with parameters determined by fitting the experimental phonon dispersion curves. For the anharmonic part he used a nearest-neighbor cubic anharmonic term with two parameters that were determined by fitting thermal expansion data. The results ob-

tained by Cowley agree reasonably well with experiment for the line shift, but are an order of magnitude too large for the linewidth. The source of this discrepancy may lie in inadequacies in the harmonic model, the anharmonic model, or other aspects of the calculation.

In the present paper we report the results of lattice dynamical calculations of the width and shift of the optical phonon line in the light scattering spectrum of intrinsic silicon as functions of temperature. The harmonic part of the lattice dynamical model includes central interactions out to and including fourth neighbors, angle-bending interactions involving pairs of nearest neighbors, and long-range nonlocal dipole interactions of the type discussed by Lax.[7] The anharmonic part of the model is restricted to cubic terms and consists of nearest-neighbor central interactions. The necessary sums over wave vector are evaluated using 770 points in the irreducible one-forty-eighth portion of the Brilloun zone. The results are compared with the experimental data of Balkanski *et al.*[5] and with the theoretical results of Cowley.[3]

II. HARMONIC MODEL

The harmonic part of the lattice dynamical model is the same as that employed by Wanser and Wallis[8] in their investigation of the thermal expansion of silicon. Included in the model are first- through fourth-neighbor central interactions, angle-bending interactions, and nonlocal dipole interactions. There are eleven parameters characterizing these interactions. One of the parameters was eliminated using the condition of static equilibrium. The remaining parameters were determined by optimizing the fit to the three elastic constants, the Raman frequency, seven normal mode frequencies at high-symmetry points on the zone boundary and the Σ_3^- mode near the K point. Details may be found in Ref. 9.

For central potential interactions of a given range, the contribution to the harmonic potential energy can be written as

$$\Phi_2^{(i)}=\tfrac{1}{4}\sum_{l,\kappa}\sum_{l',\kappa'}\sum_{\alpha,\beta}\phi_{\alpha\beta}^{(i)}(l,\kappa;l',\kappa')u_\alpha(l,\kappa;l',\kappa')u_\beta(l,\kappa;l',\kappa')\ , \tag{2.1}$$

where

$$\phi_{\alpha\beta}^{(i)}(l,\kappa;l',\kappa')=\left[\frac{r_\alpha r_\beta}{r^2}\left[\phi_i''(r)-\frac{1}{r}\phi_i'(r)\right]+\frac{\delta_{\alpha\beta}}{r}\phi_i'(r)\right]\Bigg|_{\mathbf{r}=\mathbf{R}(l,\kappa;l',\kappa')}\ , \tag{2.2}$$

$\phi_i(r)$ is the potential function for ith-neighbor interactions, (l,κ) designates the κth atom in the lth unit cell,

$$\mathbf{u}(l,\kappa;l',\kappa')=\mathbf{u}(l,\kappa)-\mathbf{u}(l',\kappa')\ , \tag{2.3}$$

$$\mathbf{R}(l,\kappa;l',\kappa')=\mathbf{R}(l,\kappa)-\mathbf{R}(l',\kappa')\ , \tag{2.4}$$

$\mathbf{u}(l,\kappa)$ is the displacement of atom (l,κ) from its equilibrium position at $\mathbf{R}(l,\kappa)$, α and β denote Cartesian components, and the primes denote derivatives with respect to argument. It should be emphasized that the indices (l,κ) and (l',κ') of a given term must be consistent with the index i. The force constant matrices for first- through fourth-neighbor interactions have the forms

$$\overleftrightarrow{\phi}^{(1)}=\begin{bmatrix}\alpha & \beta & \beta\\ \beta & \alpha & \beta\\ \beta & \beta & \alpha\end{bmatrix}\ , \tag{2.5}$$

$$\alpha=\frac{1}{3}\left[\phi_1''(r_1)+\frac{2}{r_1}\phi_1'(r_1)\right]\ , \tag{2.6a}$$

$$\beta=\frac{1}{3}\left[\phi_1''(r_1)-\frac{1}{r_1}\phi_1'(r_1)\right]\ , \tag{2.6b}$$

$$\overleftrightarrow{\phi}^{(2)}=\begin{bmatrix}\mu & \nu & 0\\ \nu & \mu & 0\\ 0 & 0 & \mu-\nu\end{bmatrix}\ , \tag{2.7}$$

$$\mu=\frac{1}{2}\left[\phi_2''(r_2)+\frac{1}{r_2}\phi_2'(r_2)\right]\ , \tag{2.8a}$$

$$\nu=\frac{1}{2}\left[\phi_2''(r_2)-\frac{1}{r_2}\phi_2'(r_2)\right]\ , \tag{2.8b}$$

$$\overleftrightarrow{\phi}^{(3)}=\begin{bmatrix}\mu' & \nu' & \delta'\\ \nu' & \mu' & \delta'\\ \delta' & \delta' & \lambda'\end{bmatrix}\ , \tag{2.9}$$

$$\mu'=\frac{1}{11}\left[\phi_3''(r_3)+\frac{10}{r_3}\phi_3'(r_3)\right]\ , \tag{2.10a}$$

$$\nu'=\frac{1}{11}\left[\phi_3''(r_3)-\frac{1}{r_3}\phi_3'(r_3)\right]\ , \tag{2.10b}$$

$$\delta'=3\nu',\quad \lambda'=\mu'+8\nu'\ , \tag{2.10c}$$

$$\overleftrightarrow{\phi}^{(4)}=\begin{bmatrix}\lambda'' & 0 & 0\\ 0 & \mu'' & 0\\ 0 & 0 & \mu''\end{bmatrix}\ , \tag{2.11}$$

$$\lambda''=\phi_4''(r_4),\quad \mu''=\frac{1}{r_4}\phi'(r_4)\ , \tag{2.12}$$

where r_i is the ith-neighbor distance. We note that r_4 is the fundamental cube edge.

The contribution of the angle-bending interactions to the potential energy can be written in the form

$$\Phi^a=\tfrac{1}{2}\sigma r_1^2\sum_{l,\kappa}\sum_{l',\kappa'}\sum_{l'',\kappa''}\Delta\theta^2(l,\kappa;l',\kappa';l'',\kappa'') \tag{2.13}$$

where $\Delta\theta(l,\kappa;l',\kappa';l'',\kappa'')$ is the change in angle between the atoms (l,κ), (l',κ'), and (l'',κ''), with (l,κ) at the vertex and $(l,\kappa),(l',\kappa')$ and $(l,\kappa),(l'',\kappa'')$ nearest-neighbor pairs. The equilibrium value of the angle θ is the tetrahedral angle—i.e., 109.47°—and σ is the angle-bending force constant.

It was pointed out many years ago by Lax[10] that long-range interactions are necessary to give a satisfactory description of the phonon dispersion curves of silicon. In particular, the flat TA branch is difficult to describe without long-range forces. Of the various ways that one can introduce long-range interactions, we have chosen

that involving nonlocal dipole moments induced on atoms by the displacements of neighboring atoms.[7] To terms linear in the displacements, the dipole moment component induced on atom $l\kappa$ can be written as

$$p_\alpha(l\kappa)=\sum_\beta \sum_{l',\kappa'} p_{\alpha\beta}(l,\kappa;l',\kappa')[u_\beta(l',\kappa')-u_\beta(l,\kappa)] \tag{2.14}$$

where $p_{\alpha\beta}(l,\kappa;l',\kappa')$ is an element of the nonlocal dipole moment tensor. We restrict ourselves to nearest-neighbor nonlocality, and under this condition, we can write

$$\vec{p}(0,0;0,1)=\begin{vmatrix} p_1 & p_2 & p_2 \\ p_2 & p_1 & p_2 \\ p_2 & p_2 & p_1 \end{vmatrix} \tag{2.15}$$

where p_1 and p_2 are parameters to be determined and have the dimension of charge.

The interaction energy for a pair of dipoles can be written as[9]

$$W(l,\kappa;l',\kappa')=\frac{1}{\epsilon_0}\sum_{\alpha,\beta}\Omega_{\alpha\beta}(l,\kappa;l',\kappa')p_\alpha(l,\kappa)p_\beta(l',\kappa') , \tag{2.16}$$

where ϵ_0 is the static dielectric constant,

$$\Omega_{\alpha\beta}(l,\kappa;l',\kappa')=\frac{\delta_{\alpha\beta}}{|\mathbf{R}(l,\kappa;l',\kappa')|^3}-\frac{3R_\alpha(l,\kappa;l',\kappa')R_\beta(l,\kappa;l',\kappa')}{|\mathbf{R}(l,\kappa;l',\kappa')|^5} , \tag{2.17}$$

and certain short-range terms have been neglected. The total dipole-dipole interaction energy is obtained by summing $W(l\kappa;l'\kappa')$ over all pairs of dipoles:

$$\Phi^{dd}=\tfrac{1}{2}\sum_{l,\kappa}\sum_{l',\kappa}{}' W(l,\kappa;l',\kappa') . \tag{2.18}$$

The total potential energy associated with the vibrations of the atoms is obtained by summing the contributions from the short-range interactions, the angle-bending interactions, and the dipole-dipole interactions. From the result,

$$\Phi=\sum_i \Phi^i+\Phi^a+\Phi^{dd} , \tag{2.19}$$

we calculate the second derivatives of Φ with respect to displacement components and obtain the elements of the dynamical matrix from the relation

$$D_{\alpha\beta}(\kappa,\kappa';\mathbf{q})=\frac{1}{M}\sum_l \Phi_{\alpha\beta}(l,\kappa;0,\kappa')e^{-i\mathbf{q}\cdot\mathbf{R}(l)} \tag{2.20}$$

where M is the atomic mass, $\mathbf{R}(l)$ is the position vector of the origin of unit cell l, and

$$\Phi_{\alpha\beta}(l,\kappa;l',\kappa')=\frac{\partial^2\Phi}{\partial u_\alpha(l,\kappa)\partial u_\beta(l',\kappa')} . \tag{2.21}$$

By diagonalizing the dynamical matrix, we obtain the normal-mode frequencies $\omega(\mathbf{q},j)$ and normal-mode eigenvectors $\mathbf{e}(\kappa;\mathbf{q},j)$.

The force constants which characterize the various interactions were determined in the manner described in the first paragraph of this section. The elastic constants and Raman frequency ω_R are related to the force constants by the expressions

$$aC_{11}=\alpha+4\sigma+8\mu+2\mu'+9\lambda'+8\lambda'' , \tag{2.22a}$$

$$aC_{12}=2\beta-\alpha-2\sigma+8\nu-4\mu-4\lambda-10\mu'+2\nu'-\lambda'+12\delta'-8\mu'' , \tag{2.22b}$$

$$aC_{44}=\alpha+\tfrac{2}{3}\sigma+4\mu+4\lambda+\lambda'+10\mu'+8\mu''-\frac{(4\sigma/3-\beta+2\delta'+3\nu')^2}{\alpha+8\sigma/3+2\mu'+\lambda'} , \tag{2.22c}$$

and

$$\omega_R^2=(1/M)(8\alpha+64\sigma/3+16\mu'+8\lambda') . \tag{2.23}$$

It is interesting to note that the nonlocal dipole parameters p_1 and p_2 do not enter into the expressions for the elastic constants and the Raman frequency. This is in contrast to the local quadrupole-quadrupole interactions used by Lax,[10] where the quadrupole parameter enters into the elastic constants and ω_R. The longitudinal and transverse acoustical frequencies at the X and L points, the longitudinal and transverse optical frequencies at the L point, and the transverse optical frequency at the X point were also employed in the force constant determination. The expressions for these frequencies are rather

TABLE I. Force constants and nonlocal dipole parameters for the harmonic model.

$\alpha=4.7008\times10^4$ dyne/cm
$\beta=3.0364\times10^4$
$\mu=5.4455\times10^3$
$\nu=4.7303\times10^3$
$\lambda=(\mu-\nu)=7.1520\times10^2$
$\sigma=4.3265\times10^3$
$\mu'=-2.2679\times10^3$
$\nu'=-8.0545\times10$
$\lambda'=(\mu'+8\nu')=-2.9122\times10^3$
$\delta'=3\nu'=-2.4164\times10^2$
$\lambda''=9.9978\times10$
$\mu''=-\frac{1}{8}(\alpha-\beta+8\mu-8\nu+11\mu'-11\nu')=2.1190\times10^2$
$Z_1=0.804\,905$, $Z_2=-0.201\,226$, $(Z_2/Z_1)=-0.25$ with $p_1=Z_1e$ and $p_2=Z_2e$
e is the electron charge in CGS units
$\phi_1''(r_0)=(\alpha+2\beta)=1.0774\times10^5$ dyne/cm
$\frac{\phi_1'(r_0)}{r_0}=(\alpha-\beta)=1.6644\times10^4$
$\phi_2''(r_2)=(\mu+\nu)=1.0176\times10^4$
$\frac{\phi_2'(r_2)}{r_2}=\lambda=7.1520\times10^2$
$\phi_3''(r_3)=(\mu'+10\nu')=-3.073\times10^3$
$\frac{\phi_3'(r_3)}{r_3}=(\mu'-\nu')=-2.1873\times10^3$
$\phi_4''(a)=\lambda''=9.9978\times10$
$\frac{\phi_4'(a)}{a}=\mu''=2.1190\times10^2$

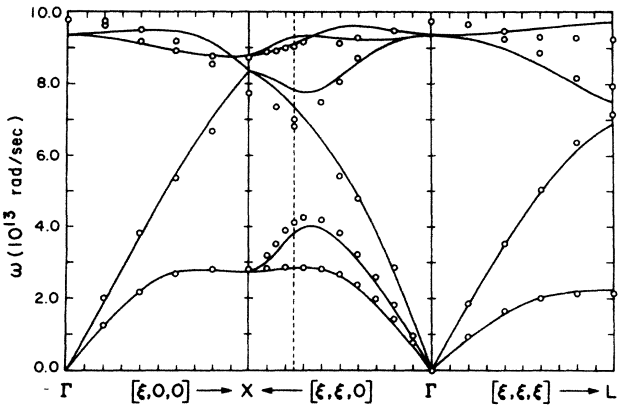

FIG. 1. Phonon dispersion curves for silicon obtained experimentally (circles) and theoretically (solid curves). The experimental points are from G. Dolling, in *Inelastic Scattering of Neutrons in Solids and Liquids* (IAEA, Vienna, 1963), Vol. II, p. 37; G. Dolling, in *Inelastic Scattering of Neutrons*, Vol. I (IAEA, Vienna, 1965), p. 249; G. Nilsson and G. Nelin, Phys. Rev. B 6, 3777 (1972). The theoretical curves are calculated using the model described in the text.

complicated because of the nonlocal dipole contribution and will not be given here. They can be found in Ref. 9. The results for the force constants and nonlocal dipole parameters taken from Ref. 9 are listed in Table I, and the calculated phonon dispersion curves based on these values are given in Fig. 1 together with the experimental data. We see that the agreement between the experimental and theoretical curves is very good. The nonlocal dipole interactions play a key role in obtaining a satisfactory fit for the transverse acoustic branches.

III. ANHARMONIC MODEL

The harmonic model employed in this work can be generalized in a straightforward fashion to include cubic anharmonic terms. One introduces thereby a number of cubic anharmonic force constants which must be determined by fitting experimental values of third-order elastic constants, mode Grüneisen parameters, thermal expansion, and other appropriate experimental data. This procedure is complicated by the possibility of inner displacements in crystals with the diamond structure. In the present report we do not consider the entire set of cubic anharmonic force constants associated with the first- through fourth-neighbor central interactions, the angle-bending interactions, and the dipole-dipole interactions. Instead, we restrict our attention to nearest-neighbor central interactions. This enables us to provide a rather direct comparison with the work of Cowley[3] and also, it turns out, leads to a reasonably good value for the linewidth.

By considering various types of elastic deformations, one can establish relations between the third-order elastic constants and the cubic anharmonic force constants. With nearest-neighbor central interactions, we have only one parameter to determine, namely, $\phi_1'''(r_1)$. We have employed an isotropic deformation in which the finite strain tensor element $\eta_{\alpha\beta}$ is specified by

$$\eta_{\alpha\beta}=\eta\delta_{\alpha\beta}\ . \tag{3.1}$$

The elements $\eta_{\alpha\beta}$ are related to the elements $\epsilon_{\alpha\beta}$ of the linear strain tensor by

$$\eta_{\alpha\beta}=\tfrac{1}{2}(\epsilon_{\alpha\beta}+\epsilon_{\beta\alpha})+\tfrac{1}{2}\sum_{\lambda}\epsilon_{\lambda\alpha}\epsilon_{\lambda\beta} \tag{3.2}$$

where

$$\epsilon_{\alpha\beta}=\frac{\partial u_\alpha}{\partial x_\beta}\ . \tag{3.3}$$

The relation of $\phi_1'''(r_1)$ to the second and third-order elastic constants is given by

$$\phi_1'''(r_1)=(4/\sqrt{3})(C_{111}+6C_{112}+2C_{123}+3C_{11}+6C_{12})\ , \tag{3.4}$$

where we have used the Voigt notation for the elastic constants. To the best of our knowledge, this relation for $\phi_1'''(r_1)$ has not been previously given in the literature. It provides a convenient way of determining $\phi_1'''(r_1)$ from the experimental elastic constants, since $\phi_1''(r_1)$ and $\phi_1'(r_1)$, which appear in the latter, have cancelled out. Using the experimental values of the second- and third-order elastic constants given by McSkimm and Andreatch,[11] we obtain

$$\phi_1'''(r_1)=-6.416\times10^{13}\ \text{dyn/cm}^2\ . \tag{3.5}$$

This value is in reasonable agreement with that calculated independently from mode Grüneisen parameters.[9]

IV. FOURIER-TRANSFORMED ANHARMONIC COEFFICIENTS

An essential ingredient of the calculation of the Raman spectrum is the set of Fourier-transformed anharmonic coefficients that enter into the expressions for the phonon proper self-energy. The contribution of cubic anharmonic terms to the potential energy of the crystal can be written in the following form if we restrict ourselves to two-body central interactions,

$$\Phi_3=\tfrac{1}{12}\sum_i\sum_{l,\kappa}\sum_{l',\kappa'}\sum_{\alpha,\beta,\gamma}\phi^{(i)}_{\alpha\beta\gamma}(l,\kappa;l',\kappa')u_\alpha(l,\kappa;l',\kappa')u_\beta(l,\kappa;l',\kappa')u_\gamma(l,\kappa;l',\kappa')\ , \tag{4.1}$$

where i specifies the interaction between ith neighbors and

$$\phi^{(i)}_{\alpha\beta\gamma}=\left[\frac{r_\alpha r_\beta r_\gamma}{r^3}\left(\phi_i'''(r)-\frac{3}{r}\phi_i''(r)+\frac{3}{r^2}\phi_i'(r)\right)+\frac{r_\alpha\delta_{\beta\gamma}+r_\beta\delta_{\alpha\gamma}+r_\gamma\delta_{\alpha\beta}}{r^2}\left(\phi_i''(r)-\frac{1}{r}\phi_i'(r)\right)\right]\Bigg|_{\mathbf{r}=\mathbf{R}(l,\kappa;l',\kappa')}\ . \tag{4.2}$$

As in the case of the harmonic potential energy, the indices (l,κ) and (l',κ') must be consistent with the index i.

The Fourier-transformed anharmonic coefficients are obtained by taking the normal coordinate transformation

$$u_\alpha(l\kappa)=\sum_{\mathbf{q},j}[\hbar/2NM_\kappa\omega(\mathbf{q}j)]^{1/2}e_\alpha(\kappa;\mathbf{q}j)e^{i\mathbf{q}\cdot\mathbf{R}(l)}A_{\mathbf{q}j}\ , \tag{4.3}$$

where N is the number of unit cells and $A_{\mathbf{q}j}$ is the normal coordinate, and substituting it into Eq. (4.1). The result can be written in the form

$$\Phi_3=\sum_{\mathbf{q},j}\sum_{\mathbf{q}',j'}\sum_{\mathbf{q}'',j''}V(\mathbf{q},j;\mathbf{q}',j';\mathbf{q}'',j'')A_{\mathbf{q}j}A_{\mathbf{q}'j'}A_{\mathbf{q}''j''}\ , \tag{4.4}$$

where

$$\begin{aligned}V(\mathbf{q},j;\mathbf{q}',j';\mathbf{q}'',j'')=\tfrac{1}{12}\sum_i\sum_{l,\kappa}\sum_{l',\kappa'}\sum_{\alpha,\beta,\gamma}&(\hbar/2NM_\kappa)^{3/2}\phi^{(i)}_{\alpha\beta\gamma}(l,\kappa;l',\kappa')\\&\times[\omega(\mathbf{q},j)\omega(\mathbf{q}',j')\omega(\mathbf{q}'',j'')]^{-1/2}[e_\alpha(\kappa;\mathbf{q},j)e^{i\mathbf{q}\cdot\mathbf{R}(l)}-e_\alpha(\kappa';\mathbf{q},j)e^{i\mathbf{q}\cdot\mathbf{R}(l')}]\\&\times[e_\beta(\kappa;\mathbf{q}',j')e^{i\mathbf{q}'\cdot\mathbf{R}(l)}-e_\beta(\kappa';\mathbf{q}',j')e^{i\mathbf{q}'\cdot\mathbf{R}(l')}]\\&\times[e_\gamma(\kappa;\mathbf{q}'',j'')e^{i\mathbf{q}''\cdot\mathbf{R}(l)}-e_\gamma(\kappa';\mathbf{q}'',j'')e^{i\mathbf{q}''\cdot\mathbf{R}(l')}]\ .\end{aligned} \tag{4.5}$$

It can be shown[1] that $V(\mathbf{q},j;\mathbf{q}',j';\mathbf{q}'',j'')$ is proportional to the quantity $\Delta(\mathbf{q}+\mathbf{q}'+\mathbf{q}'')$ where $\Delta(\mathbf{q})$ is unity if $\mathbf{q}$ is zero or a vector of the reciprocal lattice and is zero otherwise.

In many calculations of the properties of anharmonic crystals, it is necessary to evaluate sums over wave vector of the Fourier transformed anharmonic coefficient (or its magnitude squared) multiplied by various functions of wave vector. These computations are rather complex and are frequently simplified by approximating the quantities $V(\mathbf{q},j;\mathbf{q}',j';\mathbf{q}'',j'')$ by simpler expressions. For example, in the Peierls approximation,[12] one writes

$$\begin{aligned}&V(\mathbf{q},j;\mathbf{q}',j';\mathbf{q}'',j'')\\&\quad\simeq C[\omega(\mathbf{q},j)\omega(\mathbf{q}',j')\omega(\mathbf{q}'',j'')]^{+1/2}\Delta(\mathbf{q}+\mathbf{q}'+\mathbf{q}'')\ ,\end{aligned} \tag{4.6}$$

where C is a constant. This is clearly a drastic simplification of Eq. (4.5), and unfortunately does not give an accurate picture of the dependence of the V coefficient on the wave vector. We have avoided such approximations and have calculated the V coefficients in accordance with Eq. (4.5).

To illustrate the situation, we present the results for $V(\mathbf{0},j;\mathbf{q},j';-\mathbf{q},j'')$ for several cases. When the index j refers to an optical branch ($j=4,5,6$), these anharmonic coefficients are those that appear in the damping constant and frequency shift for the Raman mode. In the first case, we plot in Fig. 2(a) the coefficients $V(\mathbf{0},4;\mathbf{q},3;-\mathbf{q},3)$ and $V(\mathbf{0},5;\mathbf{q},3;-\mathbf{q},3)=V(\mathbf{0},6;\mathbf{q},3;-\mathbf{q}3)$ as functions of wave vectors $\mathbf{q}=(0.5,\zeta,\zeta)2\pi/a$ for $0.0\le\zeta\le0.5$. The branch indices $j=3$, 4, 5, and 6 refer to the longitudinal acoustical branch, the two transverse optical branches, and the longitudinal optical branch, respectively. We see that the V coefficients start from zero at $\zeta=0.0$, increase until they reach maximum values of ~0.40 at $\zeta\sim0.375$, and then decrease rapidly. The second case concerns wave vectors specified by $\mathbf{q}=(0.5,\zeta,0.0)2\pi/a$, and the results for $V(\mathbf{0},6;\mathbf{q},3;-\mathbf{q},3)$ are presented in Fig. 2(b). This coefficient starts from zero at $\zeta=0.0$, increases monotonically and reaches its maximum value at $\zeta=0.5$. The coefficients $V(\mathbf{0},4;\mathbf{q},3;-\mathbf{q},3)$ and $V(\mathbf{0},5;\mathbf{q},3;-\mathbf{q},3)$ are both zero for $0.0\le\zeta\le0.5$ in this case. The last case corresponds to $\mathbf{q}=(0.5,0.5,\zeta)2\pi/a$ and is presented in Fig. 2(c). The coefficient $V(\mathbf{0},6;\mathbf{q},3;-\mathbf{q},3)$ starts at its maximum value at $\zeta=0.0$ and decreases monotonically to its minimum value at $\zeta=0.5$. The value of $V(\mathbf{0},4;\mathbf{q},3;-\mathbf{q},3)=V(\mathbf{0},5;\mathbf{q},3;-\mathbf{q},3)$ starts at zero, reaches a maximum at $\zeta\sim0.25$ and decreases thereafter.

When the Peierls approximation is used to calculate the V coefficients in the above cases, the coefficients are found to increase monotonically with increasing ζ in all three cases. The percentage increases in the coefficients from $\zeta=0.0$ to $\zeta=0.50$ are 25%, 17%, and 15%, respectively. The qualitative behavior of the coefficients is therefore rather different from that found using the exact expressions. Furthermore, we have established that in the case of 2LA[ζ00] decay, the V coefficient including terms out to fourth-neighbor central interactions is zero for all ζ, so the Peierls approximation is drastically in error in this case.

V. SCATTERING EFFICIENCY

In the present work, we focus on Stokes scattering by zone-center LO phonons in silicon. The differential scattering efficiency for incident frequency ω_I and scattered frequency ω_S is given by[5]

$$\frac{d^2S}{d\omega\, d\Omega}=\frac{e^4LV}{2\pi\hbar^3m^4a^2MNc^4\omega(0,j)}\left[\frac{\omega_S}{\omega_I}\right][n(\omega)+1]\times|R(j,IS)|^2\frac{\Gamma(0j;\omega)}{[\omega-\Omega(0,j;\omega)]^2+\Gamma^2(0,j;\omega)}\ , \tag{5.1}$$

where $R(j,IS)$ is the Raman tensor, the branch index j refers to the longitudinal optical branch, a is the lattice constant, L and V are the crystal thickness and volume, respectively, $\omega(0,j)$ is the zone-center LO-phonon frequency, $n(\omega)$ is the thermal occupation factor given by

$$n(\omega)=\frac{1}{e^{\hbar\omega/k_BT}-1}\ , \tag{5.2}$$

and m is the free-electron mass.

The resonant frequency $\Omega(0j,\omega)$ in Eq. (5.1) specifies the line position of the scattered radiation and is given to first approximation by

$$\Omega(0,j;\omega)=\omega(0,j)+\Delta(0,j;\omega)\ . \tag{5.3}$$

The quantities $\Delta(0,j;\omega)$ and $\Gamma(0,j;\omega)$ are proportional to the real and imaginary parts, respectively, of the phonon proper self-energy, $P(0,j;\omega)$, as expressed by the relation[1]

$$\lim_{\epsilon\to0^+}P(0,j;\omega+i\epsilon)=-\beta\hbar[\Delta(0,j;\omega)-i\Gamma(0,j;\omega)]\ , \tag{5.4}$$

where $\beta=1/k_BT$. In general, the proper self-energy at $\mathbf{q}=0$ is a matrix $P_{jj'}$; however, it can be shown for silicon that $P_{jj'}$ is diagonal. We shall refer to $\Delta(0,j;\omega)$ as the frequency shift and $\Gamma(0,j;\omega)$ as the damping constant of the mode $(0,j)$. These quantities can be expressed as sums of contributions arising from cubic, quartic and higher-order terms in the anharmonic Hamiltonian. In the present paper we restrict our attention to second-order cubic anharmonic terms arising from nearest-neighbor central interactions and corresponding to the diagram in Fig. 3(a). Second-neighbor, fourth-neighbor, and all higher-even-neighbor central interactions do not contribute to $\Delta(0,j;\omega)$ and $\Gamma(0,j;\omega)$ for the Raman mode of silicon, because they involve interactions between pairs of atoms on the same sublattice. The expressions for $\Delta(0,j;\omega)$ and $\Gamma(0,j;\omega)$ are

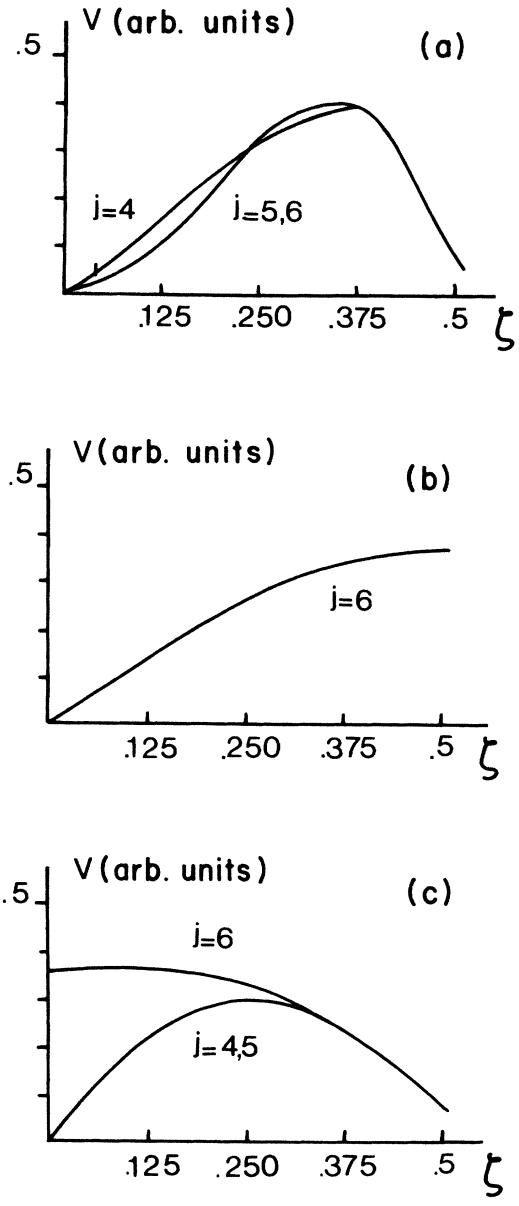

FIG. 2. (a) Anharmonic coefficients $V(0,4;\mathbf{q},3;-\mathbf{q},3)$ and $V(0,5;\mathbf{q},3;-\mathbf{q},3)=V(0,6;\mathbf{q},3;-\mathbf{q},3)$ as functions of $\mathbf{q}=(0.5,\zeta,\zeta)2\pi/a$ for $0.0\le\zeta\le0.5$. (b) Anharmonic coefficient $V(0,6;\mathbf{q},3;-\mathbf{q},3)$ as a function of $\mathbf{q}=(0.5,\zeta,0.0)2\pi/a$. (c) Anharmonic coefficients $V(0,4;\mathbf{q},3;-\mathbf{q},3)=V(0,5;\mathbf{q},3;-\mathbf{q},3)$ and $V(0,6;\mathbf{q},3;-\mathbf{q},3)$ as functions of $\mathbf{q}=(0.5,0.5,\zeta)2\pi/a$. The quantity a is the edge of the fundamental cube.

$$\Delta(0,j;\omega)=-\frac{18}{\hbar^2}\sum_{\mathbf{q}}\sum_{j_1,j_2}|V(0,j;\mathbf{q},j_1;-\mathbf{q},j_2)|^2\mathscr{P}\left[\frac{n_1+n_2+1}{\omega+\omega_1+\omega_2}-\frac{n_1+n_2+1}{\omega-\omega_1-\omega_2}+\frac{n_1-n_2}{\omega-\omega_1+\omega_2}-\frac{n_1-n_2}{\omega+\omega_1-\omega_2}\right] \tag{5.5}$$

$$\Gamma(0,j;\omega)=\frac{18\pi}{\hbar^2}\sum_{\mathbf{q}}\sum_{j_1,j_2}|V(0,j;\mathbf{q},j_1;-\mathbf{q},j_2)|^2\times\{(n_1+n_2+1)[\delta(\omega-\omega_1-\omega_2)-\delta(\omega+\omega_1+\omega_2)]+(n_1-n_2)[\delta(\omega+\omega_1-\omega_2)-\delta(\omega-\omega_1+\omega_2)]\} \tag{5.6}$$

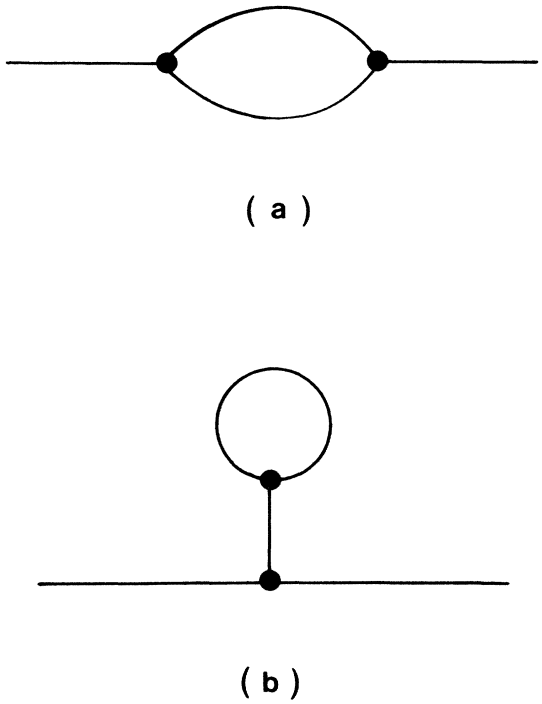

FIG. 3. Feynman diagrams for second-order cubic anharmonic contributions to the phonon proper self-energy.

where $\mathscr{P}$ denotes the principal value and

$$\omega_i=\omega(\mathbf{q},j_i),\quad i=1,2,3,4,5,6 \tag{5.7a}$$

$$n_i=\frac{1}{e^{\beta\hbar\omega_i}-1},\quad i=1,2,3,4,5,6\ . \tag{5.7b}$$

There are additional contributions in principle to $\Delta(\mathbf{0},j;\omega)$ and $\Gamma(\mathbf{0},j;\omega)$ that arise from the diagram in Fig. 3(b) and which involve the product of anharmonic coefficients

$$V(\mathbf{0},j;\mathbf{0},j;\mathbf{0},j_1)V(\mathbf{0},j_1;\mathbf{q},j_2;-\mathbf{q},j_2)\ .$$

For a crystal with every atom at a center of inversion, both factors in the above product are zero.[1] Silicon has a center of inversion midway between the two atoms of the unit cell, but not at an atomic site itself; consequently, neither of the two factors need be zero. One can show, however, that the left-hand factor is zero unless the branch indices j and j_1 both refer to optical branches. We have calculated the value of this factor using our model for all possible combinations of j and j_1 corresponding to optical branches and find that it is zero even in this case. The coefficient $V(\mathbf{0},j;\mathbf{0},j_1;\mathbf{0},j_2)$ is different from zero only when j, j_1, and j_2 refer to three different optical branches.

VI. NUMERICAL CALCULATION OF THE FREQUENCY SHIFT AND DAMPING CONSTANT

Using our harmonic and anharmonic lattice-dynamical model for silicon, we have made numerical calculations of the frequency shift $\Delta(\mathbf{0},j;\omega)$ and the damping constant $\Gamma(\mathbf{0},j;\omega)$ as functions of frequency ω and temperature T. We first calculated $\Gamma(\mathbf{0},j;\omega)$ using Eq. (5.6). The sum over $\mathbf{q}$ was evaluated by using 770 points in the irreducible one-forty-eighth portion of the Brillouin zone. The necessary representation for the δ function was chosen to have the Gaussian form

$$\delta(\omega)=\lim_{\epsilon\to 0}\left[\frac{1}{\epsilon\sqrt{\pi}}e^{-\omega^2/\epsilon^2}\right]. \tag{6.1}$$

In actual practice, ϵ must have a finite value that is sufficiently large to give a reasonable number of $\mathbf{q}$ points a nontrivial weight and yet sufficiently small that the function is sharply peaked. When these conditions are satisfied, the calculated damping constant is sensibly independent of ϵ over a range of values of ϵ. We found that $\epsilon=1.0$ Trad/s lies in the center of such a range of values and have accordingly used this value of ϵ.

Of particular importance to the Raman spectrum is the damping constant evaluated at $\omega=\omega_R$ where ω_R is the Raman frequency. We have carried out a calculation of $\Gamma(\mathbf{0},j;\omega_R)$ as a function of temperature using the procedure outlined above. Since the quantity $2\Gamma(\mathbf{0},j;\omega_R)$ is a first approximation to the full width at half maximum (FWHM) of the Raman line, we have plotted the calculated values of $2\Gamma(\mathbf{0}j;\omega)$ versus temperature in Fig. 4 together with the experimental values[5] of the FWHM. We see that the theoretical values lie roughly 30% below the experimental points at temperatures up to 500 K, but are otherwise in good qualitative agreement with the data. At temperatures above 500 K, the experimental values increase more rapidly with increasing temperature than do the theoretical values, which increase linearly with temperature at high temperatures. Possible reasons for this discrepancy will be discussed in the next section.

Also plotted in Fig. 4 are the calculated values of Cowley.[3] They are seen to be much too large compared to the experimental data. It is difficult to pin down just what the problem is with Cowley's calculations. Although the adequacy of his harmonic model (shell model) has been

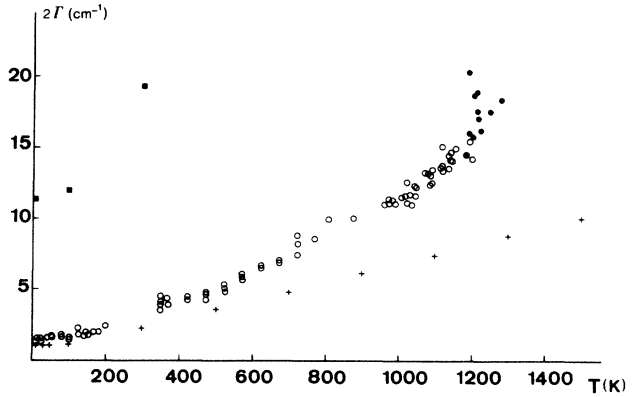

FIG. 4. Quantity $2\Gamma(\mathbf{0},j;\omega_R)$ versus absolute temperature as calculated by Cowley (solid squares) and by the present authors (crosses). The experimental data for the full width at half-height of the Raman line (Ref. 5) are represented by the open and solid circles.

questioned,[6] Cowley claims that it gives "excellent" agreement with the phonon dispersion curves determined by inelastic neutron scattering. His nearest-neighbor anharmonic model is similar to ours, but he uses the anharmonic parameters of Dolling and Cowley,[13] determined by fitting the thermal expansion. Now one can show rigorously that the B parameter of Dolling and Cowley is zero for a nearest-neighbor central potential model, in contradiction to their result that B is different from zero. Furthermore, the value of $\phi_1'''(r_1)$ can be calculated from their A parameter and is found to be $+3.09\times10^{13}$ dyn/cm^2. This result differs in sign from our value given by Eq. (3.5). For a typical interatomic potential, the quantity $\phi''(r)$ *decreases* as r increases and becomes negative as r becomes very large. Consequently, $\phi'''(r)$ is expected to be negative, in agreement with our result. In addition, ϕ_1''' must be negative to give the correct signs to the mode Grüneisen parameters and third order elastic constants. We therefore feel that our result is physically the more reasonable one.

The frequency dependence of the damping constant has been calculated at various temperatures. In Fig. 5(a) we plot the results for 10 K when the V coefficient is taken to have the form of a constant times $\Delta(\mathbf{q}+\mathbf{q}_1+\mathbf{q}_2)$, so that the damping constant is determined by an effective two-phonon density of states. The peaks can be associated with various two-phonon combinations. Thus, the broad peak around 60 Trad/s is due to 2TA, while the highest-frequency peak is due to LO-TA and TO-TA combinations.

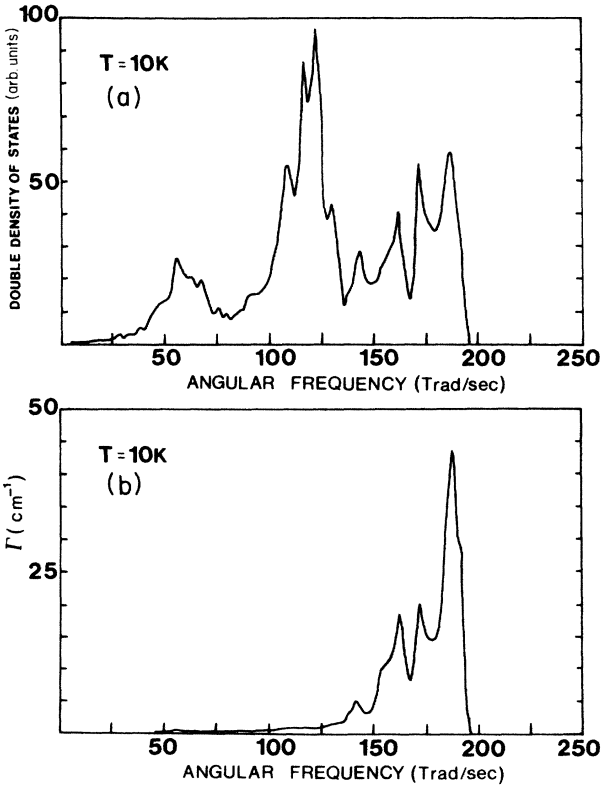

FIG. 5 Frequency dependence at 10 K of the damping constant $\Gamma(\mathbf{0},j;\omega)$ using (a) two-phonon density of states and (b) exact results for the anharmonic coefficients $V(\mathbf{0},j;\mathbf{q},j_1;-\mathbf{q},j_2)$.

When one uses the exact expression for the V coefficient, Eq. (4.5), one obtains the result shown in Fig. 5(b). It is evident that the damping constant in the low-frequency range is much reduced relative to its value in the high-frequency range. This behavior can be understood in terms of the factors in square brackets in Eq. (4.5) that involve the eigenvector components. In the low-frequency range, j' and j'' refer to acoustical modes, the eigenvector components tend to cancel in the square bracketed factors involving j' and j'', and the V-coefficient is small. In the high-frequency range, on the other hand, j' and j'' refer to optical modes, the eigenvector components tend to reinforce each other, and the V coefficient is large.

As the temperature is increased, the damping constant increases at all frequencies in the two-phonon frequency range, but the increase is more rapid in the low-frequency region than in the high-frequency region. This behavior is a consequence of the occupation factors n_1 and n_2 reaching their classical limits more rapidly for low frequencies than for high frequencies.

The other quantity of interest is the frequency shift $\Delta(0j,\omega_R)$. It may be calculated in principle from the expression given by Eq. (5.5). However, we have chosen to calculate it from the damping constant $\Gamma(\mathbf{0},j,\omega)$ by means of the Kramers-Kronig relation

$$\Delta(\mathbf{0},j;\omega_R)=\frac{1}{\pi}\int_{-\infty}^{\infty}d\omega'\frac{\Gamma(\mathbf{0},j;\omega')}{\omega_R-\omega'}\ . \tag{6.2}$$

The integral in Eq. (6.2) was evaluated numerically using the calculated values of the damping constant.

There are two additional contributions to $\Delta(\mathbf{0},j;\omega_R)$ that are proportional to T in the high-temperature limit. One arises from thermal expansion and is given by[14]

$$\Delta^E=-3\omega(\mathbf{0},j)\gamma(\mathbf{0},j)\int_0^T\alpha(T')dT' \tag{6.3}$$

where $\gamma(\mathbf{0},j)$ is the Grüneisen constant for the Raman mode and $\alpha(T)$ is the coefficient of thermal expansion. The other arises from quartic anharmonicity in first order and is given by

$$\Delta^{(4)}(\mathbf{0},j;\omega_R)=\frac{24}{\hbar}\sum_{\mathbf{q}_1,j_1}V(\mathbf{0},j;\mathbf{0},j;\mathbf{q}_1,j_1;-\mathbf{q}_1,j_1)(n_1+\tfrac{1}{2}) \tag{6.4}$$

where $V(\mathbf{0},j;\mathbf{0},j;\mathbf{q}_1,j_1;-\mathbf{q}_1,j_1)$ is a quartic anharmonic coefficient specified by a generalization[5] of Eq. (4.5).

We have used tabulated values[9] of the thermal expansion coefficient as a function of temperature to evaluate Δ^E for silicon. The results have been incorporated into the calculation of the total frequency shift $\Delta(\mathbf{0},j;\omega)$. We have neglected the quartic anharmonic contribution to Δ given by Eq. (6.4). The results for the temperature dependence of the frequency shift $\Delta(\mathbf{0},j;\omega_R)$ are presented in Fig. 6 together with the experimental data of Balkanski *et al.*[5] We see that the decrease in $\Delta(T)-\Delta(0)$ with increasing temperature as given by the theory is less than that found experimentally, particularly at temperatures above 500 K. We note that the inclusion of the thermal expansion contribution to Δ leads to improved agreement

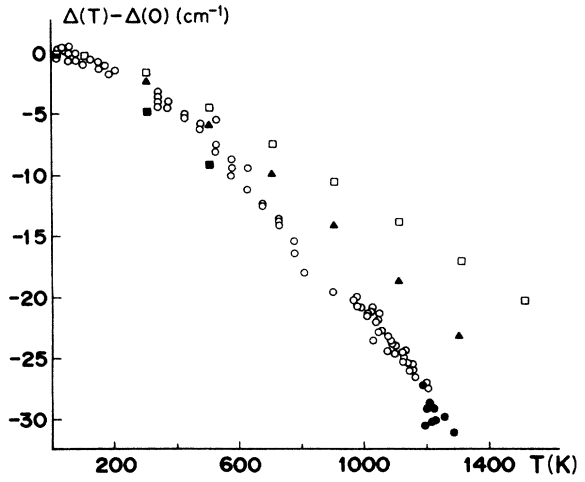

FIG. 6. Difference of the frequency shift at temperature T and at zero temperature versus temperature as calculated by Cowley (solid squares) and by the present authors; both including the thermal expansion contribution (solid triangles) and not including this contribution (open squares). The experimental data (Ref. 5) are represented by open and solid circles.

with experiment. However, Cowley[3] has stated that the quartic anharmonic contribution given by Eq. (6.4) tends to cancel the thermal expansion contribution given by Eq. (6.3), so the inclusion of the former would tend to reduce the agreement of theory with experiment. It remains to be seen whether this is in fact the case.

We have used the Kramers-Kronig relation, Eq. (6.2), to calculate the frequency dependence of the frequency shift at several temperatures. The results for 10 K are plotted in Fig. 7 and show typical dispersive behavior supplemented by fine structure. The frequency shift is negative at frequencies below ~ 185 Trad/s and is positive at frequencies above this value. At higher temperatures, the magnitude of $\Delta(0,j;\omega)$ is larger, but the qualitative behavior is little changed.

The frequency dependence of $\Delta(0,j;\omega)$ leads to an additional contribution[6] to the linewidth. To first approximation, the corrected half-width $\Gamma_c(\Omega_R)$ is given by

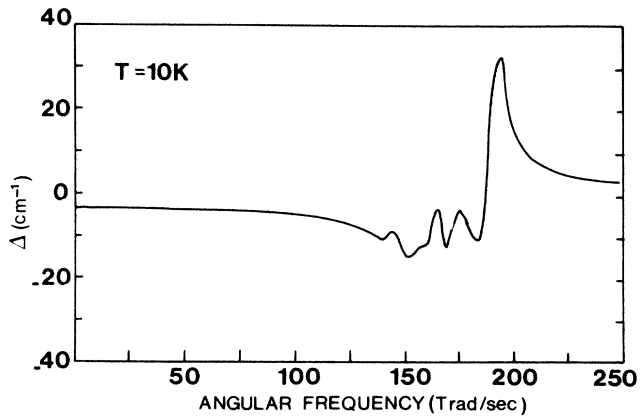

FIG. 7. Frequency dependence of the frequency shift $\Delta(0,j;\omega)$ at 10 K.

$$\Gamma_c(\Omega_R)=\frac{\Gamma(0,j;\Omega_R)}{1-\Delta_1}\ , \tag{6.5}$$

where Ω_R is the conventional center of the Raman peak specified by

$$\Omega_R=\omega(0,j)+\Delta(0,j;\Omega_R) \tag{6.6}$$

and

$$\Delta_1=\frac{d\Delta(0,j;\Omega)}{d\Omega}\Big|_{\Omega=\Omega_R}\ . \tag{6.7}$$

From our calculated values of $\Delta(0,j;\Omega)$ we find that $\Delta_1\sim -0.01$ at the Raman frequency, so the correction to the linewidth specified by Eq. (6.5) is on the order of 1%.

VII. DISCUSSION

The temperature dependences of the damping constant and linewidth that have been calculated and reported in this paper are in reasonably good agreement with the experimental data and represent a significant advance over the early results of Cowley. However, there are ways in which our calculations can be improved. For example, the harmonic model which we used can be improved by the addition of quadrupole-quadrupole and quadrupole-nonlocal dipole interactions.[9] Alternatively, one could use the bond-charge model[15] which gives a very good fit to the experimental phonon-dispersion curves. However, the use of the bond-charge model to investigate anharmonic properties of silicon has not been entirely successful.[16]

Our anharmonic model can be improved by including further-neighbor central interactions, angle-bending interactions, and nonlocal dipole interactions. For the case of cubic anharmonicity, the required parameters can be determined by fitting available values of third-order elastic constants, mode Grüneisen parameters, and the thermal expansion coefficient. Such a modification of the anharmonic model should lead to significantly improved agreement between theory and experiment for the temperature dependence of the linewidth and line shift at temperatures up to 500 K. For the line shift, it is also necessary to include the quartic anharmonic term given by Eq. (6.4).

In the temperature region above 500 K, it seems clear that the fourth-order cubic anharmonic terms and second-order quartic anharmonic terms must be included in the calculation of the linewidth and line shift. Since the cubic anharmonic coefficients can be regarded as known, the evaluation of the fourth-order cubic contributions is straightforward, but laborious. The evaluation of the quartic anharmonic coupling constants is complicated by the incomplete availability of values for fourth-order elastic constants and higher-order mode Grüneisen parameters. Recourse can be made to quantities such as the heat of sublimation, but more experimental information is needed to pin down all the fourth-order force constants. Another possibility is to use *ab initio* calculated values of the fourth-order coupling constants similar to those which have been calculated for diamond.[17]

Another mechanism which can contribute to the

linewidth and line shift, particularly in the high-temperature region, are the interactions of electrons and holes with optical phonons. The thermal production of electron-hole pairs increases rapidly with increasing temperature and may lead to significant contributions to the linewidth and line shift.

ACKNOWLEDGMENT

The work of one of the authors (R.F.W.) was supported in part by National Science Foundation under Grant No. DMR-85-17634.

---

*Permanent address.

[1]R. F. Wallis, I. P. Ipatova, and A. A. Maradudin, Fiz. Tverd. Tela (Leningrad) **8**, 1064 (1966) [Sov. Phys.—Solid State **8**, 850 (1966)]; I. P. Ipatova, A. A. Maradudin, and R. F. Wallis, Phys. Rev. **155**, 882 (1967).

[2]T. R. Hart, R. L. Aggarwal, and B. Lax, Phys. Rev. B **1**, 638 (1970).

[3]R. A. Cowley, J. Phys. (Paris) **26**, 659 (1965).

[4]P. G. Klemens, Phys. Rev. **148**, 845 (1966).

[5]M. Balkanski, R. F. Wallis, and E. Haro, Phys. Rev. B **28**, 1928 (1983).

[6]J. Menéndez and M. Cardona, Phys. Rev. B **29**, 2051 (1984).

[7]M. Lax, *Symmetry Principles in Solid State and Molecular Physics* (Wiley, New York, 1974).

[8]K. H. Wanser and R. F. Wallis, J. Phys. (Paris) Colloq. **42**, C6-128 (1981).

[9]K. H. Wanser, thesis, University of California, Irvine, 1982 (unpublished).

[10]M. Lax, J. Phys. Chem. Solids **8**, 422 (1959); Phys. Rev. Lett. **1**, 133 (1958); *Lattice Dynamics,* edited by R. F. Wallis (Pergamon, Oxford, 1965), p. 179.

[11]H. J. McSkimm and P. Andreatch, Jr., J. Appl. Phys. **35**, 2162 (1964).

[12]R. E. Peierls, *Quantum Theory of Solids* (Oxford University Press, Oxford, 1955), p. 38.

[13]G. Dolling and R. A. Cowley, Proc. Phys. Soc., London **88**, 463 (1966).

[14]W. J. Borer, S. S. Mitra, and K. V. Namjoshi, Solid State Commun. **9**, 1377 (1971).

[15]W. Weber, Phys. Rev. B **15**, 4789 (1977).

[16]A. P. Mayer and R. K. Wehner, Phys. Status Solidi B **126**, 91 (1984).

[17]H. D. Vanderbilt, S. G. Louie, and M. L. Cohen, Phys. Rev. Lett. **53**, 1477 (1984).